Appl. Phys. A 80, 1501–1504 (2005)
DOI: 10.1007/s00339-005-3205-5

Applied Physics A
Materials Science & Processing

C.G. KUO[1,✉]
Y.Y. HSU[2]
M.K. WU[2]
C.G. CHAO[1]

Characterization of lead-bismuth eutectic nanowires

[1] Department of Material Sciences and Engineering, National Chaio Tung University, Hsinchu 300, Taiwan, R.O.C.
[2] Institute of Physics, Academia Sinica, 128 Sec. 2, Academia Rd., Nankang, Taipei 115, Taiwan, R.O.C.

Received: 12 November 2004/Accepted: 20 December 2004
Published online: 17 February 2005 •

ABSTRACT In this work, lead-bismuth eutectic alloy nanowires were fabricated by a novel vacuum melting method and centrifugal process. An anodic aluminum oxide (AAO) template was used to produce an array of ordered, dense, and continuous Pb-Bi nanowires. Scanning electron microscopy and transmission electron microscopy investigations reveal that nanowires with a diameter of 80 nm are composed of Pb_7Bi_3 and Bi phases, and have a single orientation of growth. Magnetic susceptibility and hysteresis measurements have been used to characterize the superconductive and magnetic properties of the nanowires. The results show that Pb-Bi nanowires have a slightly lower superconducting transition temperature than Pb-Bi eutectic alloy bulk, and only about 1% superconductivity volume fraction in magnetic fields both perpendicular and parallel to the plate. In magnetization curves, a fairly large hysteresis is observed for both field orientations.

PACS 81.07.Bc; 81.20.-n; 74.70.Ad

1 Introduction

During the past decade, nanostructured materials have attracted great attention in the scientific and industrial fields. The special properties of low-dimensional systems have been researched and applied to nanotechnological applications [1].The preparation of nanowire with different materials has inspired a wide range of possible applications.

Superconductive materials have been investigated since the twentieth century. Attempts to use superconductors for the windings of solenoid magnets have been made after superconductivity was discovered by Onnes [2] in 1911. In 1930 de Haas and Voogd [3] conducted studies using Pb-Bi alloys, called “hard” superconductors, and they reported critical fields as large as 20 KGauss. Superconductors are often classified as “hard” or “soft”. This classification apparently originated from a close association with their mechanical properties.

During the 1980s, long filaments of Pb-Bi and Pb-Sn system alloys were produced, whose critical temperature (Tc) was higher than that of the bulk form. For example, $Pb_{45}Bi_{35}Sn_{20}$ and $Pb_{45}Bi_{40}Te_{15}$ filaments with a high Tc of 10.1 K and 10.2 K were obtained [4, 5]. Tanaka [6] showed that several kinds of superconducting wires, such as Nb-Ti alloy wires, Nb_3Sn compound wires, Bismuth system wires, and Yttrium system wires, were investigated. It has recently been found that bismuth telluric nanowires [7–10] were fabricated for their thermoelectric transport properties but not for superconductivity.

Although much work has been done to date, more studies need to be conducted to ascertain the effects of nanostructure in superconductivity. The purpose of this study is to investigate the structure, superconductivity, and magnetic properties of lead-bismuth eutectic (LBE) nanowires. The lead-bismuth eutectic alloy contains 44.5 wt. % Pb and 55.5 wt. % Bi [11]. Its melting point is equal to 397.7 ± 1.5 K [12]. The Pb-Bi nanowires were fabricated using a novel technique of vacuum melting and centrifugal process, which could generate continuous, straight, and dense nanowire arrays. This procedure has several advantages as follows: (1) the composition of alloys can be controlled correctly, (2) the operating conditions are easy to operate, and (3) the process is more efficient. The morphology and structure of the resulting nanowire arrays are characterized by scanning electron microscopy (SEM) and transmission electron microscopy (TEM). Their magnetic susceptibility and hysteresis are evaluated by a superconducting quantum interference device (SQUID) magnetometer.

2 Experiments

Our method was based on the centrifugal process of melted metal. It was applied with a large force to push the metal into a template. A nanoporous alumina template was generated by anodizing a pure aluminum substrate (99.7%) in 0.3 M oxalic acid. The anodic alumina template, still attached to the Al substrate, was placed on the bottom of a titanium tube and surrounded by lead-bismuth eutectic alloy pieces. Meanwhile, the vacuum pressure of the tube was maintained at 10^{-6} Torr, using a molecular turbo pump to prevent active metal oxidation. The titanium tube was then heated up to 300 °C before it was put on the centrifuge. The centrifugal radius was 2 cm and the total mass of the titanium tube, AAO template, and metal was fixed at 10 g. The centrifugal rate was 17 000 rpm. A centrifugal force was applied to the melted alloy and the Pb-Bi nanowires formed after the melted alloy

✉ Fax: 886-3-5724727, E-mail: happyday200392@yahoo.com.tw

solidified in the AAO template with an ordering pore diameter of 80 nm and 9 μm in thickness.

The morphology and the structure of the Pb-Bi nanowires were examined with a scanning electron microscopy (SEM) and a transmission electron microscopy (TEM). SEM studies were performed on a JEOL JSM 6500F field emission scanning electron microscope. TEM investigations were conducted using a JEOL JEM 2100F field emission transmission electron microscope operating at 200 kV.

Magnetic susceptibility and hysteresis measurements were carried out by a Quantum Design, μ-metal shielded $MPMS_2$, SQUID magnetometer.

3 Results and discussion

Since liquid Pb-Bi eutectic alloy has a high surface tension (410.5 dyne/cm) at 300 °C [13], a high rotation rate was needed to force liquid Pb-Bi eutectic alloy to enter the nanochannels of the AAO template. The simplified equation [14], $P = (-2\gamma \cos\theta)/r$, could be used to estimate the extra pressure needed to form Pb-Bi nanowires of 80 nm diameter and 9 μm height. Here γ is the surface tension of the liquid Pb-Bi eutectic alloy, θ is the contact angle between the liquid Pb-Bi eutectic alloy and the AAO template, and r is the radius of nanochannel. The centrifugal force [15–19] is given by $F = mrw^2$, where m is the total mass, r is the radius of centrifugation, and w is the angular speed. We can calculate the result with the equation above. The critical rate of rotation for the formation of nanowire in the AAO is 15 963 rpm. In order to produce a dense Pb-Bi nanowire and

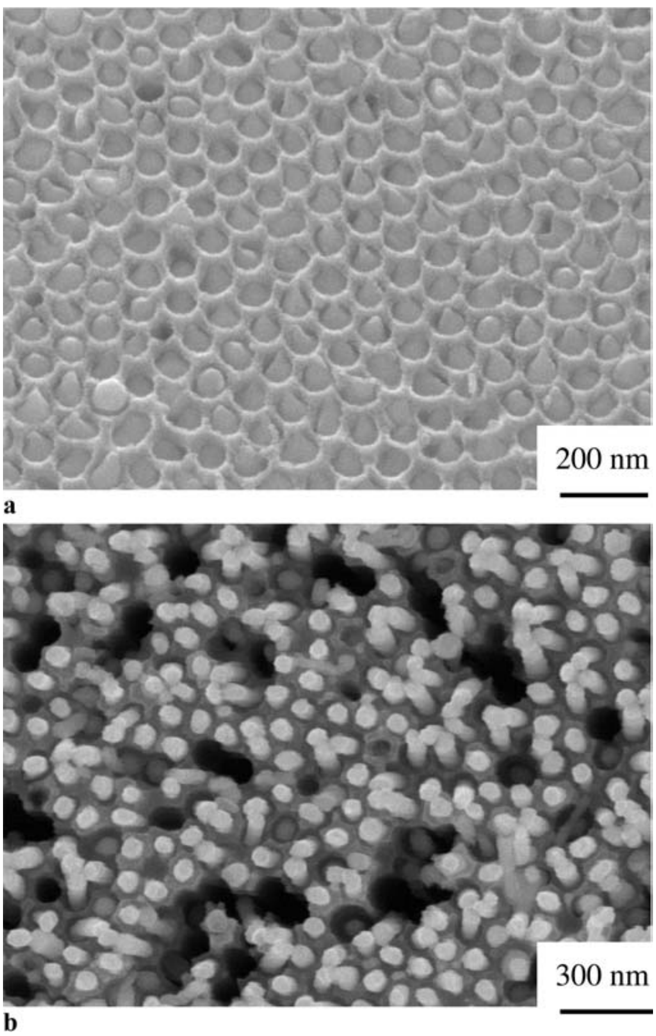

FIGURE 1 The SEM images of Pb-Bi eutectic nanowires (**a**) plane view, (**b**) top view. The rotation rate was 17 000 rpm and the Pb-Bi melt can be injected into the AAO template

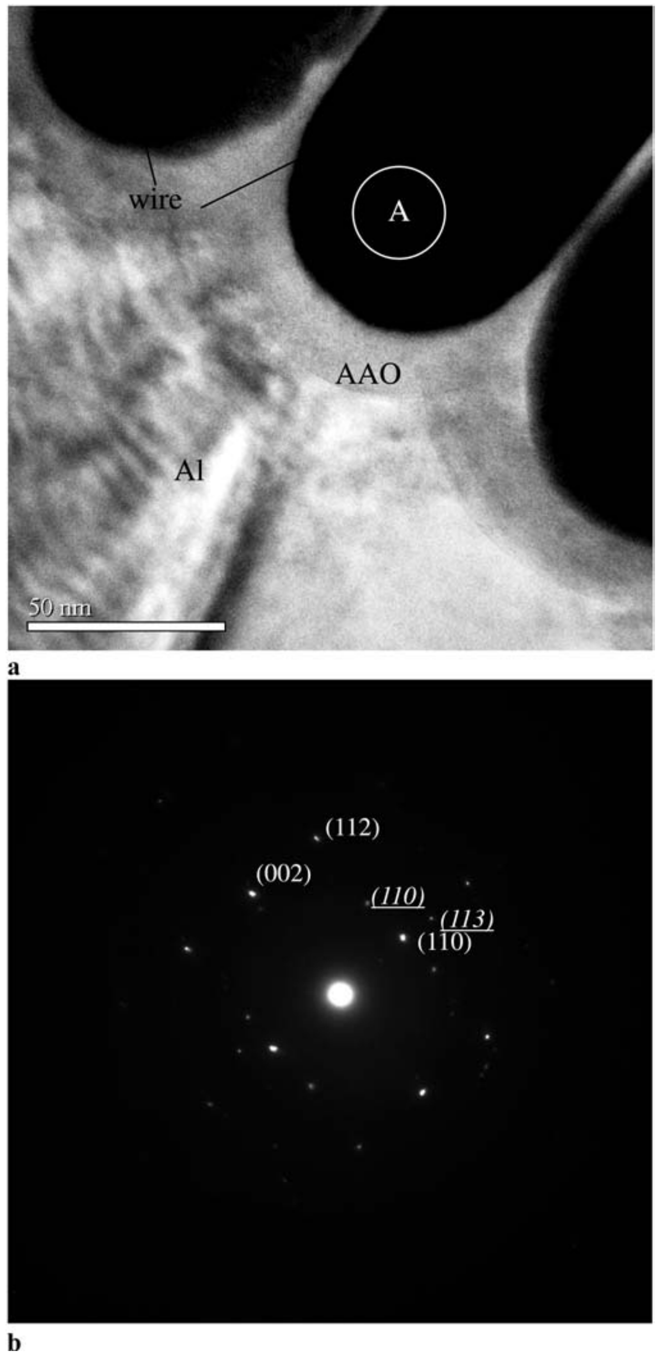

FIGURE 2 The TEM images of Pb-Bi eutectic nanowires (**a**) high-magnification TEM image of an individual Pb-Bi wire, (**b**) its electron-diffraction pattern. Indexing of the pattern established that the Pb-Bi nanowire was consistent with the [1$\bar{1}$0] zone axis of Pb_7Bi_3 and Bi (*incline* and *underline*)

improve the filling ratio, a higher rotation rate (17 000 rpm) is needed.

A SEM micrograph of Pb-Bi nanowires with the AAO template is shown in Fig. 1a which indicates that the injected metal filled the pores uniformly. The plane view image reveals that Pb-Bi nanowires with a diameter of 80 nm had an ordered and dense array. In Fig. 1b, free standing nanowire arrays were exposed from the AAO template and some voids in the figure were induced by vibration in diluted NaOH solution.

Figure 2a presents a transmission electron micrograph of a microtomed cross section of nanowire arrays. The bright field image suggests a uniform and uninterrupted wire structure where no segmentations or morphological imperfections, such as branching were observed. In addition, it also reveals that the double oxide layers of the AAO template consist of an inner oxide (barrier layer) and an outer oxide (porous layer). The thickness of the barrier layer is 17 nm. Figure 2b shows the electron-diffraction patterns produced from section A in Fig. 2a, which confirmed their single orientation of growth. In the binary phase diagrams [20], the eutectic phase of the lead-bismuth alloy consisted of the Pb_7Bi_3 and Bi phases. By way of indexing the electron diffraction patterns, there are two phases, Pb_7Bi_3 and Bi, in the Pb-Bi eutectic nanowire. In addition, both two phases have the same zone axes $[1\bar{1}0]$. In Fig. 2b the primary diffraction patterns are contributed by Pb_7Bi_3. Therefore, the results of TEM analysis correspond with the theory, and the composition of alloy nanowire can be accurately controlled by the centrifugal process.

Superconductivity was examined via magnetic measurements via a Quantum Desing $MPMS_2$ superconducting quantum interference device (SQUID) magnetometer with temperature range from 5 to 15 K. A low magnetic field of 5 Gauss was applied to avoid field suppression of the superconductivity signal. The volume of the nanowires was estimated from the SEM pictures and used for volume susceptibility estimation. Temperature dependence of the volume magnetic susceptibility $\chi_V(T)$ of Bi-Pb nanowires in the AAO template with the field parallel and perpendicular to the wires is shown in Fig. 3. The apparent diamagnetism at low temperature indicates the occurrence of superconductivity below the transition temperature $T_c \sim 8.6$ K. A slightly lower T_c value in comparison to 44.5–55.5 wt.% of Pb-Bi alloy bulk, ~ 8.8 K, may contribute to the size effect of nanowire with a diameter of ~ 80 nm, although a positional variation of composition in the wire during cooling could not be excluded. Moreover, a deviation of field cooled (FC) and zero field cooled (ZFC) curves occurs at a temperature of 8.2 K below T_c indicates an irreversibly of magnetic flux which is pinned below this temperature. The observed low superconductivity volume fraction of only about 1% in both field perpendicular and parallel to the plate may reflect large surface to volume ratio of nanowires ($\sim 1/20\ nm^{-1}$), which results the penetrated field underneath the surface skin reduce the volume fraction of superconductivity. Consequently this small volume fraction may raise the question of the origin of the magnetic flux pinning. Science the plate of the AAO template does not have a flat surface, the possibility of leaving fragment films formed by the remainence of alloy melt cannot be entirely ruled out.

Magnetization curves at different temperatures below T_c with the field parallel and perpendicular to the Pb-Bi nanowires are shown in Fig. 4a and b. The difference between

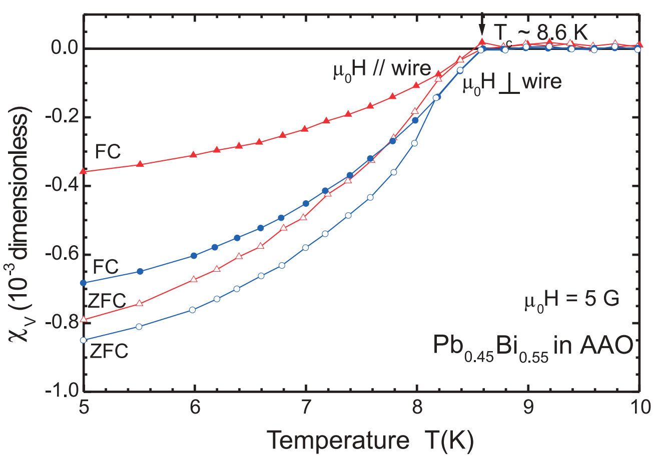

FIGURE 3 Temperature dependence of magnetic susceptibility $\chi_V(T)$ of Pb-Bi eutectic nanowires in the AAO template in zero-field-cooled (ZFC, *open symbols*) and field cooled (FC, *solid symbols*) modes with the field parallel (▲) and perpendicular (•) to the Pb-Bi eutectic nanowires. A superconducting transition was observed with transition temperature T_c around 8.6 K as indicated by the *arrow*

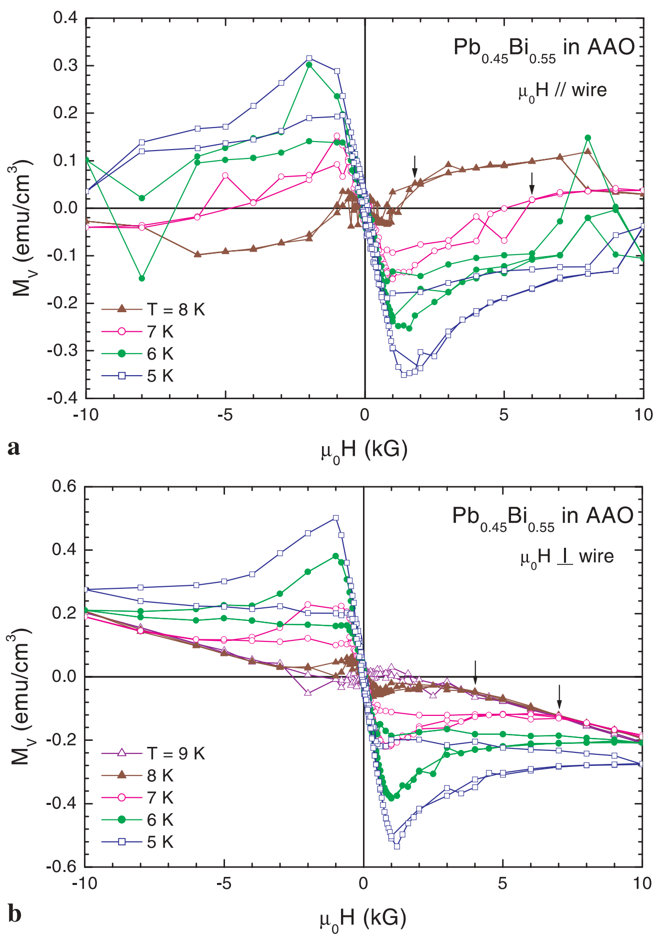

FIGURE 4 Magnetization curves, *M*–*H*, of Bi-Pb eutectic nanowires in the AAO template at different temperatures below T_c with the field parallel (**a**) and perpendicular (**b**) to the Pb-Bi eutectic nanowires. The upper critical fields are indicated by the *arrows*

different field orientations was rather qualitative and noisy for the field parallel to the wires. Due to the absence of linear parts in the initial magnetization cures, the lower critical field, $\boldsymbol{H}_{c1}$, cannot be extracted from the M–H measurement. The upper critical field, $\boldsymbol{H}_{c2}$, is indicated by arrows determined as the point where diamagnetism disappeared and the magnetization curves merge to the linear background. The $\boldsymbol{H}_{c2}$ for the field perpendicular to the Pb-Bi nanowires increases from ~ 4 kG at 7 K to ~ 7 kG at 6 K, then exceeds the maximum field (1 T) examined below 6 K. Lower $\boldsymbol{H}_{c2}(T)$ values were found for the field parallel to the wires, ~ 1.8 kG for 8 K and ~ 6 kG for 7 K. For the upper critical field at temperatures lower than 7 K, higher-applied-field measurements are required and are in progress. An almost reversible hysteresis for the field parallel to the nanowires in superconducting states at a low field region, less than about 400 G, was observed as expected for the small diameter of each individual wire. However, noticeable hysteresis was observed for the field perpendicular to the wires. Despite the qualitative difference between the two orientations at low field, a fairly large hysteresis was observed in both field orientations. The detailed flux pinning mechanism and flux dynamics in such a composite material may be quite different from bulk superconductors, as the wire's diameter and inter-wire distance are comparable to the flux sole size.

4 Conclusion

The lead-bismuth eutectic nanowires of 80 nm in diameter and 9 μm in thickness were successfully fabricated inside an AAO template by a centrifugal process. The analyses of electron diffraction patterns reveal that the Pb-Bi eutectic nanowire is composed of Pb_7Bi_3 and pure Bi phases, and each of them has the same orientation of growth. In SQUID measurements, the obvious diamagnetism at a low temperature shows that a superconducting transition occurs at a T_c of 8.6 K, which may be caused by a size effect of the Pb-Bi nanowires, and this value is a slightly lower than the bulk's. Magnetization curves at different temperatures below T_c with the field parallel and perpendicular to Pb-Bi nanowires leads to a noticeable hysteresis, observed for the field perpendicular to the wires. This study proves that some properties of Pb-Bi eutectic nanowires are different from bulk superconductors. Other properties of Pb-Bi eutectic nanowires such as optical, electric, and thermoelectric properties, will be investigated in the future.

ACKNOWLEDGEMENTS This work was supported by the National Science Council of the Republic of China under Research Contract No. NSC92-2216-E009-019.

REFERENCES

1 D. Routkeritch, A.A. Tager, J. Harayama, D. Almawlawi, M. Moskovits, J.M. Xu: IEEE Trans. Electron Devices **43**, 1646 (1996)
2 H.K. Onnes: Commun. Phys. Lab. Univ. Leiden, 120b (1911); 122b (1911); 133d (1913); 139f (1914)
3 W.J. de Hass, J. Voogd: Commun. Phys. Lab. Univ. Leiden, 208b (1930); 214b(1931)
4 T. Goto, M. Hayashi: J. J. Appl. Phys. **24**, 44 (1986)
5 T. Goto, A. Mori: J. Mater. Sci **22**, 356 (1987)
6 Y. Tanaka: Physica C**335**, 69 (2000)
7 A. Prieto, M.S. Sander, M.S. Martin-Gonzalez, R. Gronsky, T. Sands, A.M. Stacy: J. Am. Chem. Soc. **123**, 7160 (2001)
8 M.S. Sander, A.L. Prieto, R. Gronsjy, T. Sands, A.M. Stacy: Adv. Mater. **14**, 665 (2002)
9 M. Martin-Gonzalez, G.J. Snyder, A.L. Prieto, R. Gronssky, T. Sands, A.M. Stacy: Nano. Lett. **3**, 973 (2003)
10 H. Yu, P.C. Gibbons, W.E. Buhro: J. mater Chem. **14**, 595 (2004)
11 V.S. Chirkin: *The Thermophysical Properties of Materials for Nuclear Engineering Moscow* (Atomizdat 484 1968)
12 A.B. Kaplun, V.M. Shulaev, S.P. Linkov, Y.D. Vartanov: *Kutateladze Institute of the Thermophysis of the USSR* (Academy of Sciences 105 (1979))
13 B.B. Alchagirov, A.G. Mozgovoy, Kh.B. Khokonov: High Temperature **41**, 755 (2003)
14 Z. Zhang, D. Gekhtman, M.S. Dresselhaus; J.Y. Ying: Chem. Mater. **11**, 1659 (1999)
15 L. Drenchev, J. Sobczak, Modelling Simul: Mater. Sci. Eng. **11**, 635 (2003)
16 V.E. Vergara, N.V. Salazar: J. Mater. Proces. Tech. **63**, 765 (1997)
17 J. Zhanga, Z. Fana: Mater. and Design **21**, 149 (2000)
18 K. Watanabe, O. Miyakawa: Biomater. **24**, 1737 (2003)
19 Y. Nishida, G. Ohira: Acta mater. **47**, 841 (1999)
20 A.R. Putna: *Metals Handbook* (8th ed. 273 1973)